Quantum dots in the GaAs/$Al_xGa_{1-x}As$ core-shell nanowires: Statistical occurrence as a function of the shell thickness

Luca Francaviglia, Yannik Fontana, Sonia Conesa-Boj, Gözde Tütüncüoglu, Léo Duchêne, Mihaela B. Tanasescu, Federico Matteini, and Anna Fontcuberta i Morral[a)]
Laboratoire des Matériaux Semiconducteurs, Institut des Matériaux, Ecole Polytechnique Fédérale de Lausanne, 1015 Lausanne, Switzerland

(Received 6 May 2015; accepted 13 July 2015; published online 22 July 2015)

Quantum dots (QDs) embedded in nanowires represent one of the most promising technologies for applications in quantum photonics. Self-assembled bottom-up fabrication is attractive to overcome the technological challenges involved in a top-down approach, but it needs post-growth investigations in order to understand the self-organization process. We investigate the QD formation by self-segregation in $Al_xGa_{1-x}As$ shells as a function of thickness and cross-section morphology. By analysing light emission from several hundreds of emitters, we find that there is a certain thickness threshold for the observation of the QDs. The threshold becomes smaller if a thin AlAs layer is pre-deposited between the GaAs nanowire core and the $Al_xGa_{1-x}As$ shell. Our results evidence the development of the quantum emitters during the shell growth and provide more guidance for their use in quantum photonics. © *2015 AIP Publishing LLC*. [http://dx.doi.org/10.1063/1.4927315]

Quantum dots (QDs) are nanoscale portions of matter exhibiting quantum confinement and therefore controllable quantized levels. They are currently investigated and used for a manifold of applications including lasers, solar cells, and quantum information processing.[1–9] The integration of QDs in one-dimensional crystals (nanowires, NWs) has increasingly gained interest because of the improvement in the photon extraction efficiency and overall functionality.[10–19] Recently, it has been shown that self-segregation processes in ternary $Al_xGa_{1-x}As$ shells lead to the observation of luminescence stemming from 3D confined excitons. Several high-resolution imaging methods have demonstrated that the $Al_xGa_{1-x}As$ shells are indeed not homogeneous and contain nanoscale Ga-rich islands.[20–22] Another explanation for the peculiar peaks in the emission spectrum from the $Al_xGa_{1-x}As$ shell has been proposed, where the luminescence could originate from recombination at lattice point defects.[23] If this would be the case, one would expect that the QD emission would be proportional to the $Al_xGa_{1-x}As$ shell volume and mainly independent of the NW cross-section morphology.

In this report, we investigate the QD formation in function of the NW shell thickness and cross-section morphology. We demonstrate that the QD occurrence does not simply scale with the $Al_xGa_{1-x}As$ shell volume and that there is a certain thickness threshold for their observation, as well as saturation in larger shells. We also show that their formation can be facilitated if the $Al_xGa_{1-x}As$ shell is not directly grown on the GaAs (110) side-facets, but instead on a thin (5 nm) AlAs predisposition layer that significantly changes the shape of the NW cross-section. Our results are based on the analysis of several hundreds of emitters and thus provide an experimentally relevant statistical representation.

The NWs were grown in a high mobility grade molecular beam epitaxy machine (MBE, DCA P600). The GaAs NW cores were obtained by the Ga-assisted method[24] on (111) silicon wafers.[25] After the core reached around 10 μm in length, the Ga flux was interrupted and the As_4 flux increased, resulting in the stopping of the axial growth. The substrate temperature was then decreased from 640 °C to 460 °C to allow the growth of high quality epitaxial $Al_xGa_{1-x}As$ shells.[26] The $Al_xGa_{1-x}As$ layers had an aluminum ratio of 33% and a thickness varying from 10 to 100 nm. A second set of NWs were grown with a 5 nm AlAs layer between the GaAs core and the $Al_xGa_{1-x}As$ shell. In both sets, the radial growth was systematically terminated with a capping layer of 5 nm of GaAs to prevent oxidation of the inner layers. Representative transmission electron microscopy (TEM) images of the cross-sections of these two types of NWs are shown in Fig. 1. The cross-sections were realized by embedding the as-grown NWs in epoxy and cleaving thin sections with an ultra-microtome.[27,28] Fig. 1(b) corresponds to the high-angle annular dark-field (HAADF) TEM image of the sample with a simple $Al_xGa_{1-x}As$ shell. Fig. 1(c) is a bright-field (BF) TEM image of an identical sample except for 5 nm of AlAs deposition prior to the $Al_xGa_{1-x}As$ layer. Both the core and external shell present a hexagonal cross-section. In the $Al_xGa_{1-x}As$ shell, one can

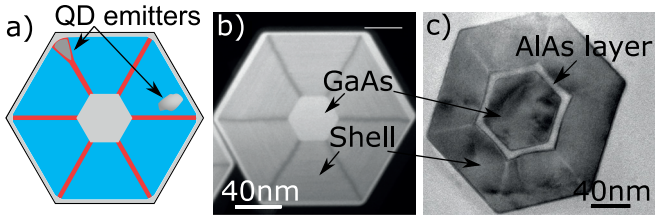

FIG. 1. (a) Sketch of a NW cross-section. The core, the shell, the Al-rich planes, and the two illustrative QDs are represented in different tones. (b) HAADF TEM image of a cross-section of a NW with simple $Al_xGa_{1-x}As$ shell. (c) BF TEM image of a cross-section of a NW with an additional 5 nm predisposition layer deposited between the GaAs core and the $Al_xGa_{1-x}As$ shell.

a)anna.fontcuberta-morral@epfl.ch

observe Al-rich regions at the six corners of the hexagon, respectively, shown as darker and brighter stripes in the dark and bright field TEM cross sections, in agreement with the previous works.[29,30] These corner features form during the shell deposition as a consequence of the inhomogeneous surface energy of the core facets, which sets element-dependent capillarity fluxes of the adatoms.[31] The corners show increased surface energy by reason of a more pronounced curvature and the presence of (112) nanofacets of higher Miller indices. Since Al shows a lower mobility than Ga, it segregates in the positions of higher energy. Noticeably, the curvature of the (110) and (112) facets of the $Al_xGa_{1-x}As$ with the GaAs core (Fig. 1(b)) is clearly different from the one with the AlAs layer (Fig. 1(c)). The meniscus shape at the $AlAs/Al_xGa_{1-x}As$ interface is consistent with more pronounced capillarity effects. This is expected for AlAs, in comparison with direct deposition of $Al_xGa_{1-x}As$ on the sharp (110) facets of the GaAs core.

Large-scale micro-photoluminescence (PL) was carried out on different NWs and along single NWs previously deposited lying on a silicon substrate. The substrate was coated with gold in order to enhance the PL signal collection. The samples were kept at 12 K on the cold finger of a helium cryostat. The 488 nm line of an ArKr laser (continuous wave) was used to optically pump the $Al_xGa_{1-x}As$ shell, leading to non-resonant excitation of the optically active QDs. The laser power was kept low (a 2 μW laser beam with energy density of about 10^2 W/cm^2) in order to prevent the observation of multiple peaks stemming from the same QD (multi-excitons and higher emission levels) and a broadening of the emission lines hindering the statistics. The collected signal was dispersed using the 600 l/mm grating of a 500 mm spectrometer and recorded on a Peltier-cooled charge-coupled device (CCD) camera. The spectra were analysed with an automatized peak finding routine and binned in a post-process step. The number of QD emission lines per spectrum was obtained through the custom routine and cast into histograms for each different sample. See supplementary material at Ref. 32 for more details about the routine and the data processing. Each histogram is the result of measuring "around" 100 NWs. As the number of QD peaks in each spectrum depends on the linear density of excited QDs in the studied NW, this approach gives an estimate of the QD linear density. This is particularly valid for a comparison among different samples even though it cannot precisely provide the absolute QD density. One should note that with this method, only the optically active QDs enter the statistics. This factually excludes segregated islands that are either too small or with low confining barrier, as carrier localization is then prevented and no light emission can originate from such nanostructures.

We now present the outcome on the density of QD emissions as a function of the shell thickness. We compare the cases where the $Al_xGa_{1-x}As$ has been deposited directly on the GaAs core and after the deposition of 5 nm of AlAs. A synthetic picture of the QD density of all samples is presented in Fig. 2. The median value of the QD peak density distributions is reported in function of the shell thickness. The upper error bar corresponds to the third quartile and the lower to the first quartile of the distributions for each kind of

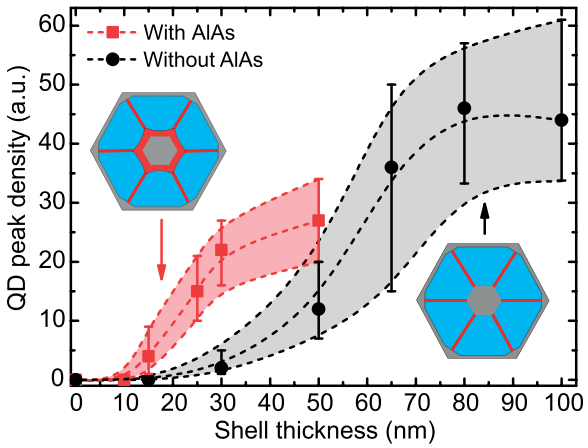

FIG. 2. Graph of the median value of PL peaks as a function of the $Al_xGa_{1-x}As$ shell thickness of all samples. Distinction is made between the two sets of samples: NWs without AlAs predisposition layer in black circles and NWs with AlAs predisposition layer in red squares. The error bars are representative of the spread of the histograms. The dashed lines are a guide to the eye.

sample, which is the spread of the histograms. The dashed lines are a guide to the eye. The resulting distributions indicate an increase of the QD density for thicker shells for both types of samples. If one focuses on the black-circle curve in Fig. 2, an interesting aspect is the non-linear increase in the density: for a thickness lower than 30 nm, almost no QD emission can be recorded. Two phenomena could be invoked to explain this behavior. First, small QDs confine the carriers wavefunction more tightly, resulting in a larger energy shift of the eigenenergies. As a result, the bound state for electrons (holes) will be shifted up (down), closer to the continuum. Since shell-QDs result from the diffusion process already mentioned,[31] it is reasonable to assume that smaller QDs also have shallower potential depth, due to higher Al content, increasing the effect further. For these reasons, luminescence from QDs smaller than 4 nm is not expected.[33] Obtaining optically active QDs in thin (15–30 nm) shells is then only possible if the nucleation rate of the QDs is high enough. For the thickest samples with, respectively, 80 and 100 nm shell, the median QD peak density seems to saturate (black-circle curve in Fig. 2). This can be understood if one considers several QDs nucleating close to each other. As the segregated islands grow, they could merge in a larger dot.

We turn now to the analysis of the QD density for the NWs with the AlAs layer between the GaAs core and the $Al_xGa_{1-x}As$ shell (red-square curve in Fig. 2). Here, the onset of QDs emission occurs for thinner $Al_xGa_{1-x}As$ shells: 15 nm in contrast to the 30 nm needed for the $Al_xGa_{1-x}As$ shell only. The unique difference between the two sets of samples is the pre-deposition of an AlAs layer, which changes the morphology of the NW cross-section. Growing a 5 nm AlAs layer on the GaAs core strongly modifies the surfaces. The 110 facets acquire a certain degree of curvature, resulting in the creation of a higher number of atomic steps. Also, the corners of the hexagonal cross-section develop rounded 112 facets. This accentuates the differences in diffusion of different adatoms and enhances segregation effects during the shell growth, which eventually seems to ease up the formation of optically active QDs.

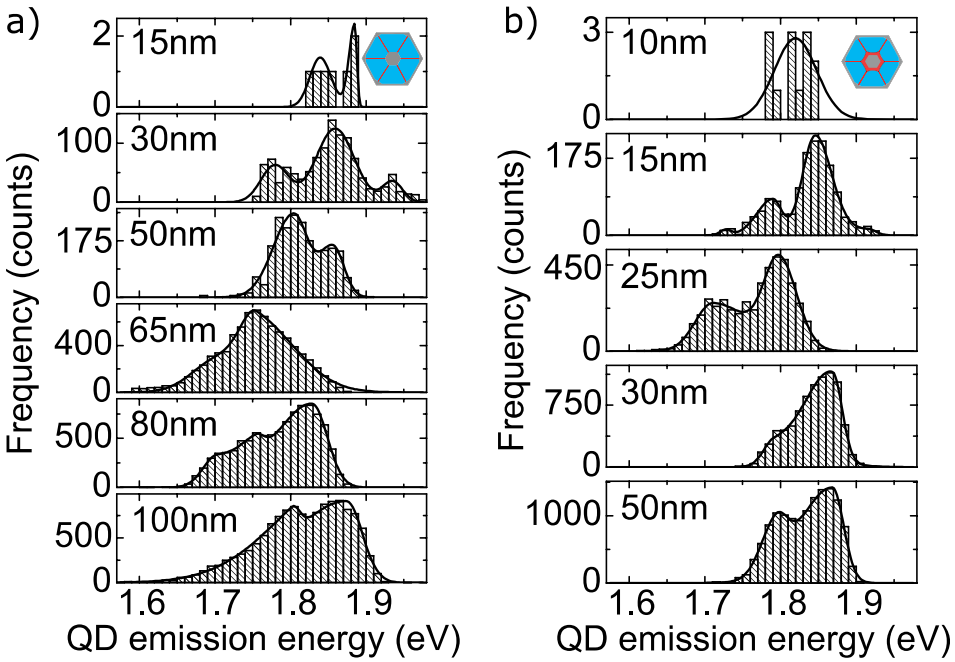

FIG. 3. Histograms of the QD emission energy as a function of the $Al_xGa_{1-x}As$ shell thickness in the case of direct growth on the GaAs core (a) and with an AlAs predisposition layer (b).

Finally, we consider the distribution of the emission energy of the QDs. Using the same dataset as before, we extract the histograms of the emission energy. In essence, this analysis should give similar results as macro-PL on a statistically representative ensemble. The advantage here is that the emission intensity is decoupled from the measurement: the histogram accounts for the presence of peaks, and not their intensity. The histograms of the QD emission energy from the two types of samples are shown, respectively, in Figs. 3(a) and 3(b) for different shell thicknesses. In both cases, the histograms develop around multiple maxima. We do not see a perfectly clear evolution of the emission with the shell thickness for all the samples with the AlAs predisposition layer. On the contrary, the other series of NWs with single $Al_xGa_{1-x}As$ shell readily shows that larger shells contain QDs with progressively red-shifted luminescence. Yet, a significant fraction of the QDs still emits at high energy, even for the 100 nm shell. We attribute this spread to the nucleation dynamics: the QD nucleation rate is not going to zero after the first QD-seeds appear. Instead, nucleation can happen at any time during the growth, giving rise to late (and small) QDs. In addition, the Ga segregated region should be fully enclosed in the $Al_xGa_{1-x}As$ matrix to be able to emit. Thus, a "closure" process, during which the $Al_xGa_{1-x}As$ can cap the segregated island, is required. We speculate that much like the nucleation process, the closure process might happen at different times during the shell growth. Upon deposition of the AlAs layer, the cross-sections evolved from a hexagonal shape to a more rounded polyhedron. This change in shape modifies the adatom mobility during the growth of the AlGaAs shell and therefore the nucleation, composition, and size of the QDs. This affects the observed emission energy.

In addition to statistical probing performed on several NWs, we realized measurements on single NWs presenting a gradient in the shell thickness. This experiment has the advantage to shed light on the effect of the shell thickness on the QD distribution directly on a single NW. The inset in Fig. 4 shows the SEM image of one of these NWs. The $Al_xGa_{1-x}As$ shell is 50 nm thicker at the top than it is at the base. The graph of QD density (squares) and average emission energy (triangles) in function of the shell thickness is also shown in Fig. 4. The dashed lines are meant as a guide to the eye. The graphs show a clear increase in QD density as the shell gets thicker, while the mean emission energy of single spectra shifts toward the red. This is verified on several NWs and proves to agree with the previous measurements performed on a larger statistical ensemble: as the shell grows thicker, the probability to nucleate QDs is expected to increase; at the same time, the energy of the observed peaks decreases significantly due to increased dimensions. This last experiment points out that the measurements made blindly on several NWs are inherently broadened. Specifically, the broadening is proportional to the tapering of the NWs, which in turn is more pronounced the higher the thickness of the sample is.

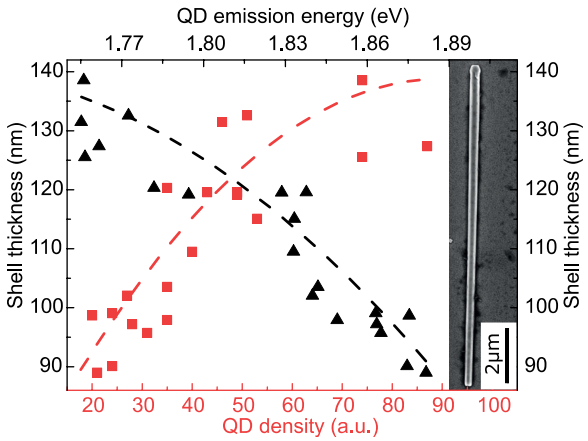

FIG. 4. Graph of QD density (squares) and local average emission energy (triangles) in function of the SEM-estimated shell thickness. Inset: SEM image of the corresponding NW without AlAs layer and with a 100 nm $Al_xGa_{1-x}As$ shell.

To summarize, we have shown that density of optically active QDs in an $Al_xGa_{1-x}As$ shell depends strongly on the shell thickness and on the nature of the underlying core. This can be easily changed from the sharp GaAs core facets into an AlAs layer that provides a different surface for the shell deposition. For a simple core/shell GaAs/$Al_xGa_{1-x}As$ structure, a cut-off in the QDs density occurs for a shell thickness of 30 nm, while it is 15 nm when an AlAs layer is predeposited on the core. We relate this cut-off to the effective growth time needed to form QDs large enough to bind excitons. The observed QD density as a function of the shell thickness confirms that the nature of the QD emission does not originate from atom-sized point-like defects but from segregations either at the corners or at the facets of the $Al_xGa_{1-x}As$ shells as recently shown by high-resolution TEM and atom probe tomography studies.[20–22]

The authors thank financial support from SNF through the NCCR QSIT and the DACH program (Grant No. 132506).

[1]D. L. Huffaker, G. Park, Z. Zou, O. B. Shchekin, and D. G. Deppe, Appl. Phys. Lett. **73**, 2564 (1998).
[2]T. Newell, D. Bossert, A. Stintz, B. Fuchs, K. Malloy, and L. Lester, IEEE Photonics Technol. Lett. **11**, 1527 (1999).
[3]P. Michler, A. Kiraz, C. Becher, W. V. Schoenfeld, P. M. Petroff, L. Zhang, E. Hu, and A. Imamoglu, Science **290**, 2282 (2000).
[4]C. Santori, D. Fattal, J. Vuckovic, G. S. Solomon, and Y. Yamamoto, Nature **419**, 594 (2002).
[5]L. Childress, J. M. Taylor, A. S. Sørensen, and M. D. Lukin, Phys. Rev. A **72**, 052330 (2005).
[6]R. M. Stevenson, R. J. Young, P. Atkinson, K. Cooper, D. A. Ritchie, and A. J. Shields, Nature **439**, 179 (2006).
[7]A. J. Nozik, Chem. Phys. Lett. **457**, 3 (2008).
[8]S. Tomić, Phys. Rev. B **82**, 195321 (2010).
[9]A. Laucht, J. M. Villas-Bôas, S. Stobbe, N. Hauke, F. Hofbauer, G. Böhm, P. Lodahl, M.-C. Amann, M. Kaniber, and J. J. Finley, Phys. Rev. B **82**, 075305 (2010).
[10]M. T. Borgström, V. Zwiller, E. Müller, and A. Imamoglu, Nano Lett. **5**, 1439 (2005).
[11]R. Agarwal and C. Lieber, Appl. Phys. A **85**, 209 (2006).
[12]E. D. Minot, F. Kelkensberg, M. van Kouwen, J. A. van Dam, L. P. Kouwenhoven, V. Zwiller, M. T. Borgström, O. Wunnicke, M. A. Verheijen, and E. P. A. M. Bakkers, Nano Lett. **7**, 367 (2007).
[13]A. Tribu, G. Sallen, T. Aichele, R. André, J.-P. Poizat, C. Bougerol, S. Tatarenko, and K. Kheng, Nano Lett. **8**, 4326 (2008).
[14]J. Heinrich, A. Huggenberger, T. Heindel, S. Reitzenstein, S. Höfling, L. Worschech, and A. Forchel, Appl. Phys. Lett. **96**, 211117 (2010).
[15]J. Claudon, J. Bleuse, N. S. Malik, M. Bazin, P. Jaffrennou, N. Gregersen, C. Sauvan, P. Lalanne, and J.-M. Gérard, Nat. Photonics **4**, 174 (2010).
[16]G. Bulgarini, M. E. Reimer, T. Zehender, M. Hocevar, E. P. A. M. Bakkers, L. P. Kouwenhoven, and V. Zwiller, Appl. Phys. Lett. **100**, 121106 (2012).
[17]S. Bounouar, M. Elouneg-Jamroz, M. d. Hertog, C. Morchutt, E. Bellet-Amalric, R. André, C. Bougerol, Y. Genuist, J.-P. Poizat, S. Tatarenko, and K. Kheng, Nano Lett. **12**, 2977 (2012).
[18]M. Montinaro, G. Wüst, M. Munsch, Y. Fontana, E. Russo-Averchi, M. Heiss, A. Fontcuberta i Morral, R. J. Warburton, and M. Poggio, Nano Lett. **14**, 4454 (2014).
[19]I. Yeo, P.-L. de Assis, A. Gloppe, E. Dupont-Ferrier, P. Verlot, N. S. Malik, E. Dupuy, J. Claudon, J.-M. Gérard, A. Auffèves, G. Nogues, S. Seidelin, J.-P. Poizat, O. Arcizet, and M. Richard, Nat. Nanotechnol. **9**, 106 (2014).
[20]M. Heiss, Y. Fontana, A. Gustafsson, G. Wüst, C. Magen, D. D. ORegan, J. W. Luo, B. Ketterer, S. Conesa-Boj, A. Kuhlmann, J. Houel, E. Russo-Averchi, J. R. Morante, M. Cantoni, N. Marzari, J. Arbiol, A. Zunger, R. J. Warburton, and A. Fontcuberta i Morral, Nat. Mater. **12**, 439 (2013).
[21]L. Mancini, Y. Fontana, S. Conesa-Boj, I. Blum, F. Vurpillot, L. Francaviglia, E. Russo-Averchi, M. Heiss, J. Arbiol, A. F. i. Morral, and L. Rigutti, Appl. Phys. Lett. **105**, 243106 (2014).
[22]Y. Fontana, P. Corfdir, B. Van Hattem, E. Russo-Averchi, M. Heiss, S. Sonderegger, C. Magen, J. Arbiol, R. T. Phillips, and A. Fontcuberta i Morral, Phys. Rev. B **90**, 075307 (2014).
[23]D. Rudolph, S. Funk, M. Döblinger, S. Morkötter, S. Hertenberger, L. Schweickert, J. Becker, S. Matich, M. Bichler, D. Spirkoska, I. Zardo, J. J. Finley, G. Abstreiter, and G. Koblmüller, Nano Lett. **13**, 1522 (2013).
[24]C. Colombo, D. Spirkoska, M. Frimmer, G. Abstreiter, and A. Fontcuberta i Morral, Phys. Rev. B **77**, 155326 (2008).
[25]E. Uccelli, J. Arbiol, C. Magen, P. Krogstrup, E. Russo-Averchi, M. Heiss, G. Mugny, F. Morier-Genoud, J. Nygard, J. R. Morante, and A. Fontcuberta i Morral, Nano Lett. **11**, 3827 (2011).
[26]M. Heigoldt, J. Arbiol, D. Spirkoska, J. M. Rebled, S. Conesa-Boj, G. Abstreiter, F. Peiró, J. R. Morante, and A. Fontcuberta i Morral, J. Mater. Chem. **19**, 840 (2009).
[27]D. C. Watson, R. V. Martinez, Y. Fontana, E. Russo-Averchi, M. Heiss, A. Fontcuberta i Morral, G. M. Whitesides, and M. Lončar, Nano Lett. **14**, 524 (2014).
[28]Q. Xu, R. M. Rioux, M. D. Dickey, and G. M. Whitesides, Acc. Chem. Res. **41**, 1566 (2008).
[29]C. Zheng, J. Wong-Leung, Q. Gao, H. H. Tan, C. Jagadish, and J. Etheridge, Nano Lett. **13**, 3742 (2013).
[30]N. Sköld, J. B. Wagner, G. Karlsson, T. Hernán, W. Seifert, M.-E. Pistol, and L. Samuelson, Nano Lett. **6**, 2743 (2006).
[31]G. Biasiol, A. Gustafsson, K. Leifer, and E. Kapon, Phys. Rev. B **65**, 205306 (2002).
[32]See supplementary material at http://dx.doi.org/10.1063/1.4927315 for representative spectra and for more details about the samples, the peak finding routine, and the QD density and energy distributions.
[33]J.-W. Luo, A. Franceschetti, and A. Zunger, Phys. Rev. B **78**, 035306 (2008).